INTENSITY OF LIGHT DIFFRACTION FROM STRIATED MUSCLE AS A FUNCTION OF INCIDENT ANGLE

R. J. BASKIN, R. L. LIEBER, T. OBA, AND Y. YEH, *Departments of Zoology and Applied Science, University of California, Davis, California 95616*

ABSTRACT In a recently developed theory of light diffraction by single striated muscle fibers, we considered only the case of normal beam incidence. The present investigation represents both an experimental and theoretical extension of the previous work to arbitrary incident angle. Angle scan profiles over a 50° range of incident angle (+25° to −25°) were obtained at different sarcomere lengths. Left and right first-order scan peak separations were found to be a function of sarcomere length (separation angle = $2\theta_B$), and good agreement was found between theory and experiment. Our theoretical analysis further showed that a myofibrillar population with a single common skew angle can yield an angle scan profile containing many peaks. Thus, it is not necessary to associate each peak with a different skew population. Finally, we have found that symmetry angle, θ_s, also varies with sarcomere length, but not in a regular manner. Its value at a given sarcomere length is a function of a particular region of a given fiber and represents the average skew angle of all the myofibril populations illuminated. The intensity of a diffraction order line is considered to be principally the resultant of two interference phenomena. The first is a volume-grating phenomenon which results from the periodic A-I band structure of the fiber (with some contribution from Z bands and H zones). The second is Bragg reflection from skew planes, if the correct relation between incident angle and skew angle is met. This may result in intensity asymmetry between the left and right first order lines.

INTRODUCTION

In a recently developed theory, we have considered the intensity changes occurring in diffraction orders resulting from the illumination of a single striated muscle fiber with a HeNe laser beam, Spectra-Physics, Inc. Mountain View, Calif.(Yeh et al., 1980). This theory, as well as our previous experiments, treated only the case where the incident laser beam was perpendicular to the muscle fiber. This approach is not sufficient to completely characterize diffraction intensities resulting from the interaction of light with a striated muscle fiber, as indicated by the following observations. First, beams diffracted to the left and right sides generally are not equally intense; second, the order-line intensities often vary with beam position along the fiber (Rüdel and Zite-Ferenczy, 1979). These observations have led to an interpretation of muscle diffraction phenomena based on Bragg reflection of light (Rüdel and Zite-Ferenczy, 1979, 1980).

To provide a satisfactory explanation of muscle diffraction based upon Bragg reflecting

---

Dr. Oba's present address is Department of Physiology, Nagoya City University Medical School, Mizuho-ku, Nagoya, 467, Japan.

planes, however, requires that each region of a muscle fiber have lattice planes with radically different tilt. Planes must be assumed to exist with tilt to both the left and right sides in order to generate both left and right order lines. Although such an assumption may occasionally hold, it appears quite restrictive to us.

We suggest that at present the most complete explanation of muscle light diffraction is given by our previously published theoretical development (Yeh et al., 1980), which includes the case where myofibrillar skew is present. Skewed A-bands can be viewed as Bragg reflecting planes. In the present investigation, muscle diffraction patterns will be analyzed using a theoretical development which treats these patterns as a result of the simultaneous

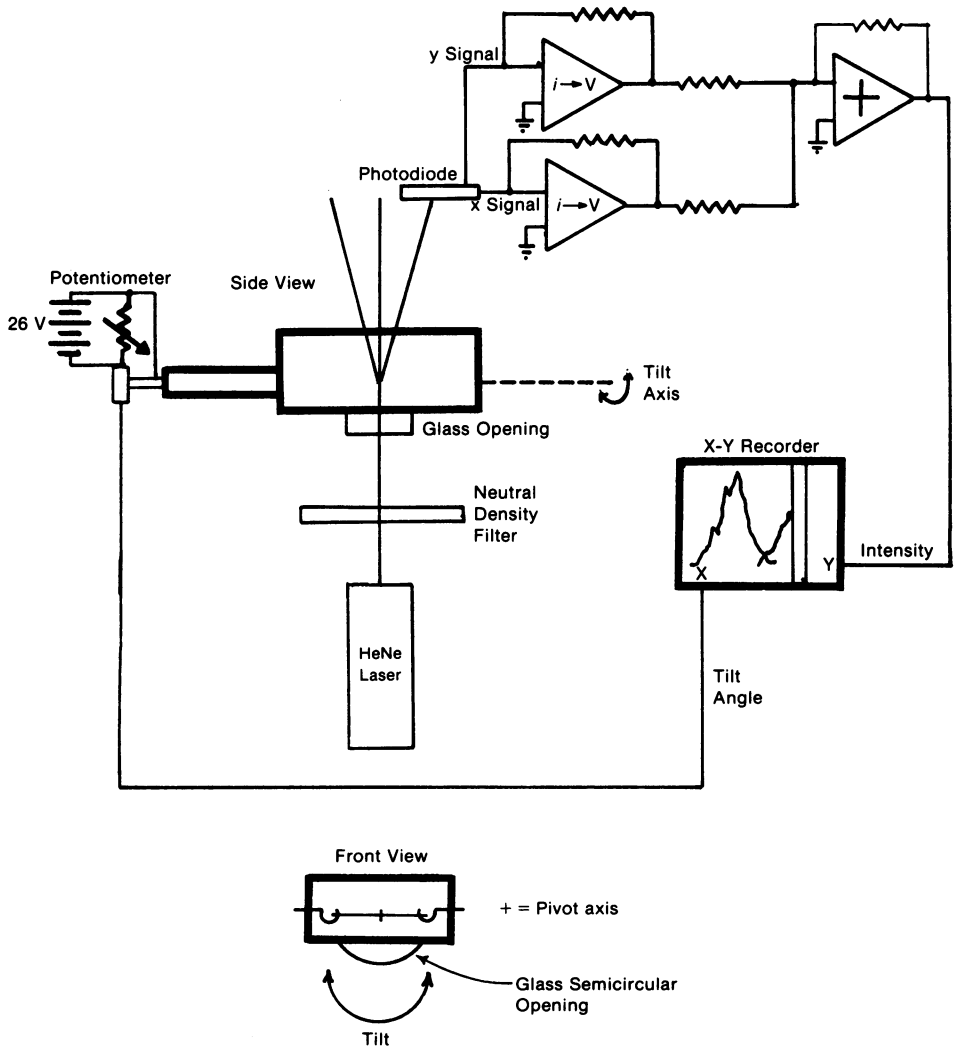

FIGURE 1 Diagram of a fiber chamber and photodiode. Chamber containing fiber rotates in a plane normal to the plane of the paper and perpendicular to the axis of the laser beam. (Diffracted orders in the "side view" are shown obliquely.)

contribution of two interference conditions. The first is described by the three-dimensional grating model. The second considers Bragg reflection from skewed A-bands as an additional interference condition. Both of these interference conditions were contained in case II of our previous study (Yeh et al., 1980). Here we will deal explicitly with the case of non-normal incidence angle. Intensity of diffraction lines will depend upon the interaction of these two interference conditions. Experimentally, we will change the angle of the fiber relative to the incident beam while measuring the intensity of the left and right first-order lines. The measured peak separations will be shown to correspond with separation angles based on a modified form of the Bragg equation.

METHODS

Single fibers from the dorsal head of the semitendinous muscle of *Rana pipiens* were used. All fibers were dissected and mounted in Ringer's solution composed of (mM): NaCl (115), KCl (2.5), Na_2HPO_4 (2.15), NaH_2PO_4 (0.85), $CaCl_2$ (1.8), and D-turbocurarine (20 mg/liter, to inhibit neuromuscular transmission during dissection). The fibers were always clear of connective and nervous tissue in the illuminated area. After dissection, the fiber was mounted in a cooled (3–5°C) aluminum chamber fitted with a glass semicircular opening through which the laser (Spectra-Physics Model 146, Mountain View, Calif.) was directed (see Fig. 1). The axis of the semicircular opening was mounted exactly on the pivot axis of the chamber. Thus, during an angle scan (defined below), no movement or attenuation of the incident beam occurred due to refraction, as the beam was always normal to the glass opening. Throughout the experiment (~3 h), chilled Ringer's solution (3–5°C) was circulated in the chamber.

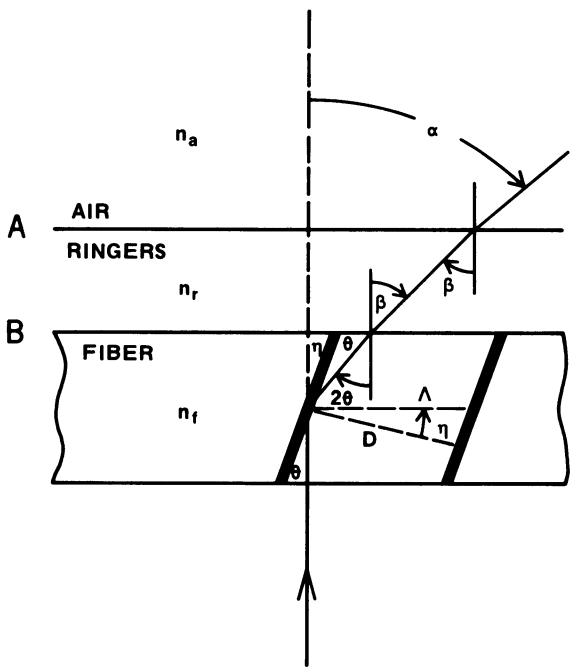

FIGURE 2 Definition of angles for a fiber with skew, η, incident light normal to the fiber axis. θ, angle of diffracted order in fiber; β, angle of diffracted order into Ringer's; α, angle of diffracted order into air; n_a, refractive index of air; n_r, refractive index of Ringer's; n_f, refractive index of fiber; Λ, sarcomere length; and D, lattice spacing.

Optical Detector System

We used a position sensitive, planar diffused photodiode as a detector (model PIN-SC/10D, United Detector Technology, Inc., Santa Monica, Calif.). The photodiode was configured so that the output voltage of the detector system was proportional to the intensity of the incident light. This was accomplished by feeding each of the four leads of the photodiode into a transresistance (current-to-voltage) amplifier and the resulting voltages into a summing amplifier. The transresistance amplifier and addition circuitry were experimentally determined to be accurate to 0.34%. The photosensitive area of the photodiode was 10.2 × 10.2 mm, but in practice was masked down so that the actual photosensitive area was a 3 × 10.2 mm slit. This increases the signal-to-noise ratio by decreasing the level of background light.

The output of the detector circuitry was fed into the Y-axis of an X-Y plotter (model F-5000, Varian Associates, Palo Alto, Calif.). The X-axis was used to measure tilt angle. This was done by attaching a variable resistor to the rotating shaft of the fiber chamber. A DC signal was applied across the potentiometer, and the voltage resulting from tilt of the chamber (rotation of the shaft) was input to the X-axis. The relationship between tilt angle and X-axis deflection was determined using a protractor mounted on the chamber. The output of the potentiometer was slightly nonlinear with tilt (error ~2° at incident angles $>\pm 18°$); thus, all absolute angle measurements (θ_s and peak separation values) were taken from the calibration sheet. The horizontal axes were labeled linearly throughout for convenience. The chamber could be repeatedly set to a given angle with an accuracy of 1° while the precision of the angle scale (ability of the plotter to detect an angle change) was about 0.1° over the range of ±35°. The photodetector system thus provided a plot of tilt angle vs. intensity (angle scan).

Determining Sarcomere Length from a Diffraction Angle Measured after Refraction

We apply Snell's law to interfaces A and B in Fig. 2 to develop a relationship between the measured diffraction angle (α) and the Bragg angle (θ). (See also Kawai, 1971, Fig. 26.)

$$n_f \sin 2\theta = n_r \sin \beta$$

$$n_r \sin \beta = n_a \sin \alpha.$$

$$\text{Since } n_a = 1,\ n_f \sin 2\theta = \sin \alpha. \tag{1}$$

The diffraction equation for the first order is:

$$\lambda = a \sin \phi \tag{2}$$

where λ = wavelength in diffracting medium, a = one-dimensional periodicity, ϕ = scattering angle. Applied to a muscle fiber where Λ = sarcomere length and λ_0 = laser wavelength in air (0.633 μm), and assuming normal incidence,

$$\frac{\lambda_0}{n_f} = \Lambda \sin 2\theta. \tag{3}$$

From Eq. 1,

$$\lambda_0 = \Lambda \sin \alpha. \tag{4}$$

[This result is due to the fact that wavelength correction ($\lambda = \lambda_0/n_f$) is the same as the angle correction ($\sin 2\theta = \sin \alpha/n_f$).]

Determination of Theoretical Bragg Angle

To compute the theoretical Bragg angle for a given sarcomere length, it is necessary first to determine the relationship between lattice spacing (D) and sarcomere length (Λ) (see Fig. 2). For a beam incident normal to the fiber where η = skew angle,

$$D = \Lambda \cos \nu. \tag{5}$$

Substituting Λ from Eq. 5 into Eq. 3, and noting that at normal incidence $\eta = \theta$,

$$\lambda_0 = \frac{D}{\cos \theta} n_f \sin 2\theta$$

$$\frac{\lambda_0}{n_f} = 2D \sin \theta. \tag{6}$$

Eq. 6 is used to compute the theoretical Bragg angle, given lattice spacing. Eq. 3 is used to compute the theoretical Bragg angle, given sarcomere length.

Experimental Protocol

The initial experiments were designed to test whether the optical system previously used (see Appendix, Baskin et al., 1979; Roos et al., 1980) was necessary to accurately measure diffracted intensity from a passive fiber. Since the working distance of the 1.4-N.A. collector lens was small (1.3 mm), the fiber could only be tilted to ±10 before the fiber hit the lens. It thus was necessary to find a fiber whose intensity peaks occurred within this range. All subsequent experiments were performed without the lens system, the photodetector placed 35 mm above the fiber.

For the duration of an angle scan, the fiber remained centered in the incident beam; lateral displacement of only 200 μm resulted in significantly different angle scans that were not readily repeatable. Therefore, before an angle scan was used for calculations, repeatability was established. For example, eight consecutive angle scans were performed on the fiber shown in Fig. 3 *a* and *b*. In addition, as the chamber was mounted on an *X-Y* manipulator, it was set so that the incident beam illuminated the fiber exactly on the point represented by the intersection of the fiber axis and the pivot axis of the chamber. This ensured that the same region of the fiber was illuminated throughout the scan. Furthermore, in changing sarcomere length, the fiber was stretched at both ends, ensuring that the same region of the fiber was illuminated at each sarcomere length.

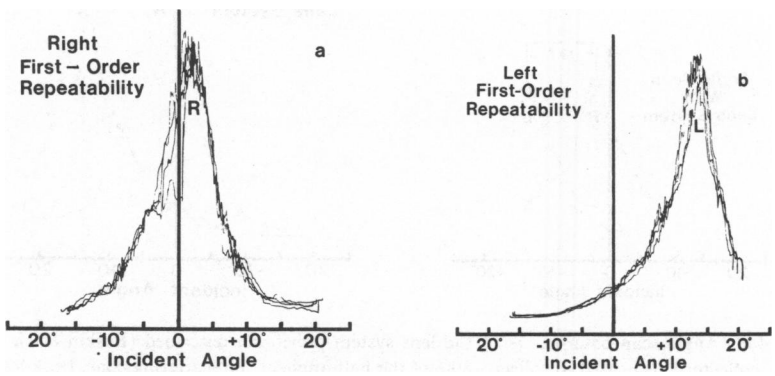

FIGURE 3 Repeatability of angle scans. (*a*) Four separate angle scans were made for a right first-order line. (*b*) Four separate angle scans from a left first-order line. Repeatability is seen to be excellent. (Sarcomere length ≃ 2.4 μm.)

RESULTS

Angle Scan with and without Lens System

The initial angle scans were performed at a given sarcomere length using the lens system described previously (Baskin et al., 1979). Angle scans were also performed without the lens system, and the results compared. Although the lens system collected 80% of the half angle of the scattering cone and without the lens system only about 10% was collected, nevertheless, as can be seen in Fig. 4 *a* and *b*, peak location and separation were identical. It is evident that for this sort of measurement, the lens system is not required. Accordingly, the remainder of our experiments were performed without the lens system.

Angle Scan As a Function of Sarcomere Length

After aligning a single fiber in the laser beam and setting the sarcomere length, the angle scan was performed. The chamber containing the fiber was rotated over a 50° range from +25° to −25°. Scans were recorded sequentially for both left and right first order diffraction line intensities.

Scans for different sarcomere lengths are presented in Fig. 5 *a-f*. Peak separation for the left and right first-order angle scans and symmetry angle θ_s was determined as described above. The symmetry angle is defined as the angle at which the left and right first order angle scans intersect. The measured peak separation was compared with the theoretical peak separation from the Bragg equation: $\lambda_0/n_f = \Lambda \sin 2\theta$, where Λ is defined as the sarcomere length (not the lattice spacing).

Peak intensity, scan profile, and symmetry angle were different for each sarcomere length. They also varied from fiber to fiber and, in some cases, with position along a given single fiber. The only feature of the left and right first order angle scan that is consistent for a given sarcomere length is the peak separation angle which is equal to $2\theta_B$.

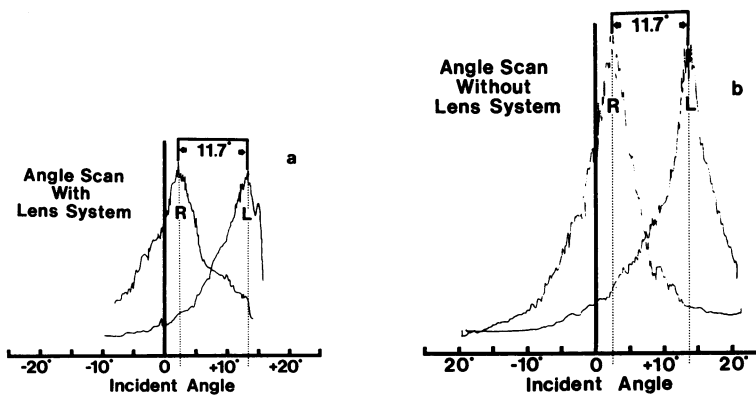

FIGURE 4 *a* Angle scan obtained using the lens system previously described (Baskin et al., 1979). A 1.4-N.A. collector lens is used to collect ~80% of the half-angle of the scattering cone. Peak location and peak separation are identical to that shown in Fig. 4 *b*. (Fig. 4 *b* was obtained without using the lens system. Sarcomere length ≃ 2.4 μm.)

FIGURE 4 *b* Angle scan obtained by collecting ~10% of the half-angle of the scattering cone. (Lens system not used.) Peak location and separation are identical to that observed using the lens system.

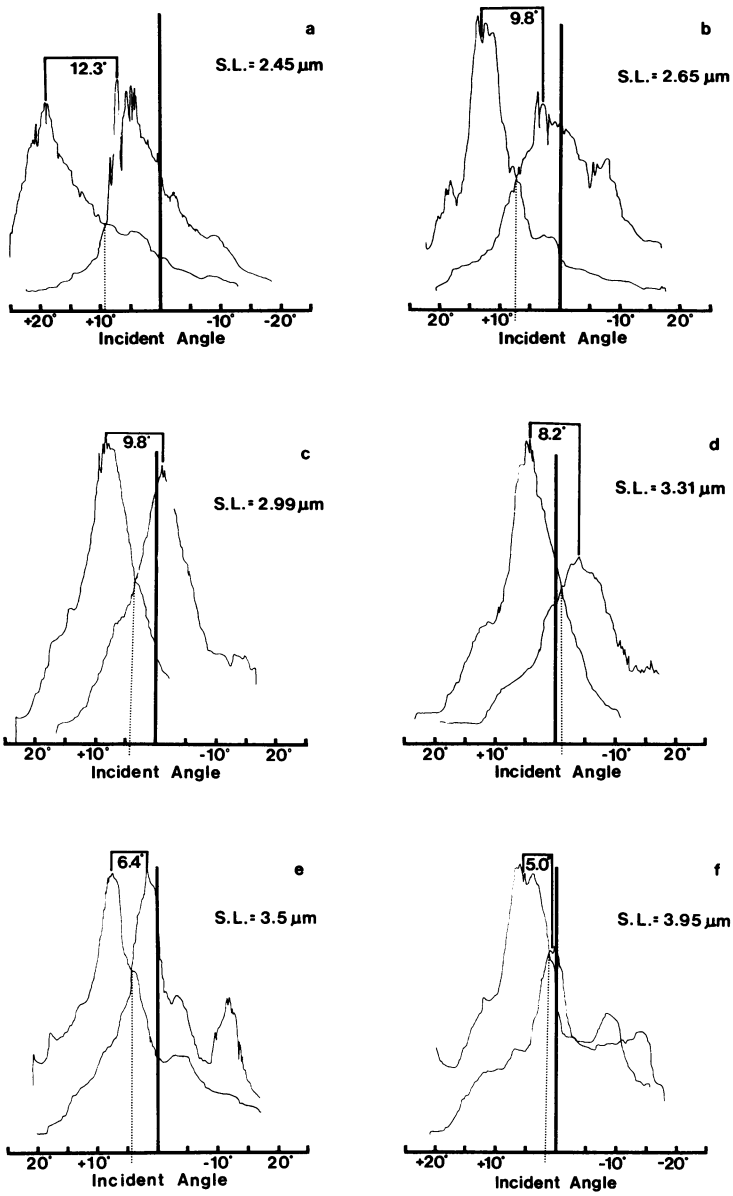

FIGURE 5 Angle scans as a function of sarcomere length. (*a*) Sarcomere of the single fiber was 2.45 μm. Symmetry angle, θ_s, was +9.0°. (*b*) Sarcomere length, 2.65 μm; symmetry angle, θ_s, +7.5°. (*c*) Sarcomere length, 2.99 μm; symmetry angle, θ_s, +4.5°. (*d*) Sarcomere length, 3.31 μm; symmetry angle, θ_s, −1.0°. (*e*) Sarcomere length, 3.50 μm; symmetry angle; θ_s, +4.0°. (*f*) Sarcomere length, 3.95 μm; symmetry angle, θ_s, +2.0°.

Peak separation was plotted as a function of sarcomere length (Fig. 6). Each point is taken from an angle scan profile at a given sarcomere length. The unconnected points represent measurements from 14 different single fibers. The connected points were taken sequentially from a single fiber. Also plotted in the same figure are the theoretical values determined from Eq. 6. Excellent agreement is observed between the theoretical and the experimental values. It is clear that peak separation angles in angle scan profiles are predictable.

Angle Scan Profiles Derived from Theory

A computer program was developed to allow the rapid solution of equations which predict diffracted intensity (Appendix A) for various values of incident angle, sarcomere length, and myofibrillar skew. (We have considered only the case of one uniform skew plane throughout the fiber, which has, however, variable thickness.) Fig. 7 is a theoretical angle scan profile, calculated (Appendix A) for a fiber with a 2.4-μm sarcomere length and a skew plane at an angle of 5.7°. The first feature to note is that the major peaks, which represent the variation with incident angle of the left and right first order lines, show a separation of $2\theta_B$, where θ_B is calculated for a sarcomere length of 2.4 μm. The second feature to note is that the secondary peaks are not separated by $2\theta_B$. They arise, in this case, solely from the thick grating nature of the model. In an experimentally determined angle scan, for a real fiber, secondary peaks may or may not be separated by $2\theta_B$. This is because they may represent either peaks from a second skew population, or interactions between peaks from different skew populations. Thus, a one-to-one association between peaks and skew populations is not justified. From the intersection of the left- and right-angle scans, the symmetry angle is seen to be nearly 5.7°. This angle equals η for a single skew population.

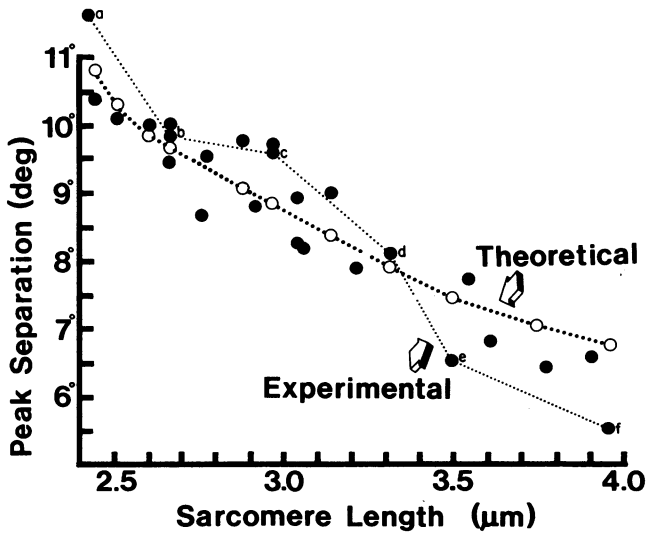

FIGURE 6 Peak separation as a function of sarcomere length for 14 single fibers. ●, experimental data. · · ·, points from the fiber in Fig. 5. ○, theoretical points computed from equation $n\lambda = 2\Lambda \sin\theta$, where Λ is the sarcomere length. Good agreement is found between the experimental data and the theoretically computed points.

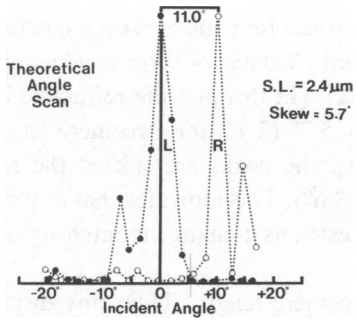

FIGURE 7

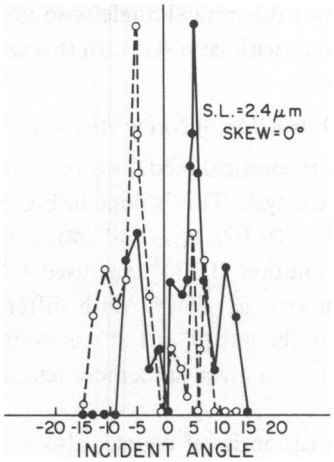

FIGURE 8

FIGURE 7 Theoretical angle scan. Sarcomere length is 2.40 μm and skew (η) = 5.7°. Major peaks are seen to be separated by $2\theta_B$, however minor peaks are not. Symmetry angle θ_s = +5.7° since there is only one skew population.

FIGURE 8 Theoretical angle scan. Sarcomere length is as 2.40 μm, and skew (η) = 0°. Thus, the symmetry angle θ_s = 0. ●, right first-order line intensity; ○, left first-order line intensity.

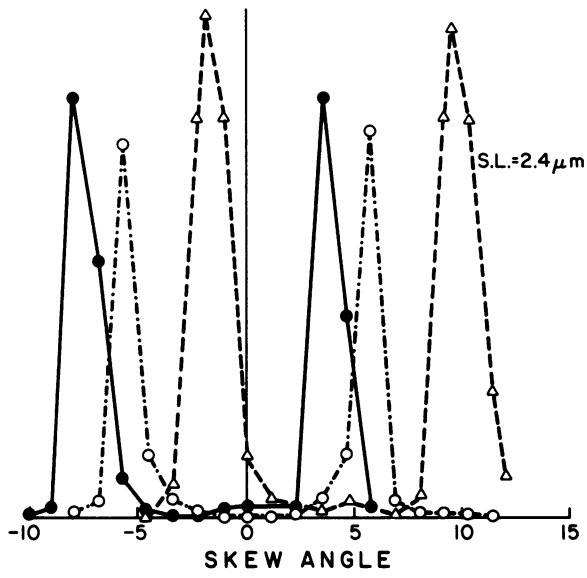

FIGURE 9

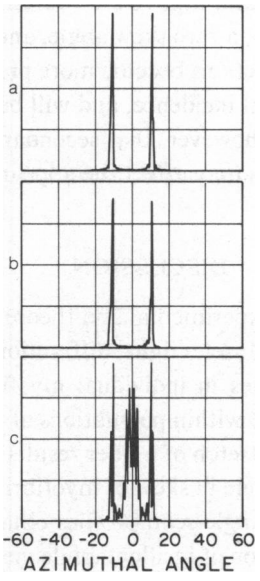

FIGURE 10

FIGURE 9 Theoretical plot; effect of skew angle on first-order line intensity. Plotted for a fiber with a sarcomere length of 2.40 μm. Points are plotted for three different angles of incidence (θ_I); 0° (○); +1.8° (●); and −3.6° (△). Note that for θ_I = 0, peaks occur at ±5.7° since that is approximately θ_B for a sarcomere length of 2.4 μm.

FIGURE 10 Intensity as a function of azimuthal angle for a fiber with a different number (N) of myofibrils. N = 1 (top), N = 10 (middle), and N = 100 (bottom). Note large light intensity appearing at and around the zero angle. This is normally masked by the undiffracted beam and is an effect of fiber thickness ("thick grating" effect).

Fig. 8 is a theoretical angle scan profile plotted for the same sarcomere length (2.40 μm), but in a fiber with zero skew. In this case $\theta_s = 0$, as expected.

Variation of Skew Angle at Constant Sarcomere Lengths

From our theoretical model we are able to plot intensity as a function of skew angle for a given sarcomere length. This is done in Fig. 9 for $\Lambda = 2.40$ μm. Values for three incident angles are plotted; $\theta_I = 0°$ (○), $\theta_I = 1.8°$ (●), and $\theta_I = -3.6°$ (△). (In this plot the refractive index for Ringer's solution [1.334] was used.) At zero θ_I, $\theta_B = 5.7°$ (2.40-μm sarcomere length), and peaks are seen at $\pm 5.7°$. With different values of θ_I, the peaks are shifted the respective amounts to the left ($\theta_I = 1.8°$) or to the right ($\theta_I = -3.6°$). This indicates that any change in skew angle at a given sarcomere length will be manifested as a change in intensity of a given order.

Peak location is, of course, also a function of sarcomere length. Thus, any dispersion of sarcomere length that is present may mask the true value of η at which maximum intensity occurs.

Effect of Grating Thickness

The thickness of a muscle fiber affects diffraction. While thick fibers contain more diffracting elements, and generally show a more intense pattern, multiple interference of undiffracted light can become an important factor. Fig. 10 *a-c* represent plots of left and right first-order line intensities for three fiber thicknesses. Fig. 10 *a* represents a 1-μm fiber, Fig. 10 *b* a 50-μm fiber, and Fig. 10 *c* a 100-μm fiber. All of the calculations were made for a 2.4-μm sarcomere length, a zero skew angle, and a normal incident beam. As fiber thickness increases, secondary interactions become more prominent, although the major effect is at zero angle for the case of normal incidence, and will be masked by the undiffracted beam (Fig. 10 *c*). It is important to note, however, that secondary effects resulting from fiber thickness do occur, and that these effects may affect the appearance of an angle scan profile.

DISCUSSION

Our experimental and theoretical results have led to the following conclusions:

(*a*) Muscle light diffraction phenomena result from an interaction between A-I band densities in individual myofibrils combined with the effects of alignment or misalignment (skew) within populations of myofibrils.

(*b*) Stretch of a fiber results in both a change in sarcomere length (A-I band periodicity) and a change in skew of myofibrils within myofibril populations.

(*c*) Angle-scan profiles obtained by measuring left and right first-order line intensities as a function of incident angle yield major peaks separated by $2\theta_B$, where θ_B is determined by using a modified form of the Bragg equation. At a given sarcomere length, the displacement from zero of the line of symmetry of the two peaks is defined as the symmetry angle, θ_s, and is a measure of the average skew of the myofibrils illuminated.

(*d*) Minor peaks need not be separated by $2\theta_B$, as they may arise from interaction between Bragg reflections from different skew populations.

Intensity Changes with Stretch

An increase in the first-order line intensity with increasing sarcomere length has been previously reported (Baskin et al., 1979), and its theoretical basis discussed (Yeh et al., 1980). It was pointed out by Rüdel and Zite-Ferenczy (1979) that this could be explained by the observation that peak separation in angle-scan profiles decreased with stretch, and that at $\omega = 0$ in their results, first-order line intensity would be expected to increase. This cannot, however, be a valid explanation for the general case of increased intensity with stretch since θ_s does not, in general, equal zero. Depending upon the value of θ_s (symmetry angle), I_{1L} or I_{1R} (see Appendix) may increase or decrease with increasing sarcomere length. Indeed, in Fig. 5 *c*, I_{1L} would decrease and I_{1R} would increase at $\omega = 0$, upon an increase in sarcomere length ($2\theta_B$ would decrease as the scan peaks moved closer together). This, however, assumes that θ_s in Fig. 5 *c* remains constant with stretch, an unwarranted assumption as shown by Fig. 5 *a-f*. The increase in intensity generally observed with increasing sarcomere length can then be explained by volume-grating diffraction by the A and I bands, and is a function of their size and relative densities with some effect of Z-band and H-zone diffraction (Yeh et al., 1980).

In general, upon stretching a resting fiber, the change in sarcomere length will result in an intensity change predicted by the volume-grating equation. Also, the skew planes of myofibrillar groups may change their skew angle, resulting in a change in average fiber skew as measured by a change in the symmetry angle (θ_s). At some sarcomere lengths the tilt of a skew plane can satisfy the Bragg condition, and a large increase in the intensity of I_{1L} or I_{1R} will be observed. (I_{1L} and I_{1R} will thus not necessarily be equally intense during stretch.)

Separation of Angle-Scan Peaks

Many angle scan profiles show a series of distinct peaks. In a recent paper Rüdel and Zite-Ferenczy (1979) identify each peak as representing a distinct population of myofibrils. As is shown in Fig. 7, however, our theoretical formulation indicates that even a fiber containing a single skew plane can generate a multipeaked angle scan profile. Such a profile is the result of the nature of the diffraction phenomena and does not necessarily indicate the existence of different skew planes (or distinct groups of myofibrils).

A single fiber is composed of groups of myofibrils, each with slightly different skew. The angle scan profile obtained from this fiber will, in general, contain a number of minor peaks. These peaks are the result of the interference of each different skew population. It is therefore not possible to associate a given minor peak with a given skew population. The separation of comparable major left and right first order scan peaks is equal to twice the Bragg angle at a given sarcomere length because the major scan peak represents an average of minor peaks which are separated by $2\theta_B$.

Origin of Muscle Diffraction

Rüdel and Zite-Ferenczy (1979, 1980) have attempted to characterize light diffraction by striated muscle as resulting from Bragg reflection of light by the protein lattice. To explain symmetrical left and right first-order lines, however, it is necessary to postulate the existence of sets of skew planes tilted at exactly opposite angles, one set for the right order lines, the other for the left. Each fiber at each sarcomere length would have to contain groups of skew planes of exactly opposite tilt. Furthermore, it is not clear why diffraction lines would not be

seen at many other locations, each corresponding to a different tilt of lattice plane. In fact, all of the major diffraction lines are found at locations given by the grating equation, computed for the fiber's sarcomere length (or average sarcomere length) in the illuminated region. We believe that this fact is owing to the basic nature of light diffraction from striated muscle.

The theoretical formulation of muscle light diffraction that we presented earlier (Yeh et al., 1980), and the supplementation included in the Appendix, predict all of the experimental results. Diffraction of light from single resting fibers is characterized by the interaction of two types of interference. One is generated by the volume-grating nature of the fiber, mainly dependent upon densities of A and I bands. It is due to this "grating" diffraction that the location of the order lines is predictable, based on the A band-I band separation (sarcomere length). Superimposed on this diffraction is a second, "Bragg reflecting plane," diffraction, that results from A-band skew in populations of myofibrils. (The implications of this phenomenon in using light diffraction to measure sarcomere length are discussed in paper by Lieber et al., submitted for publication). Depending upon the number and skew of the groups of myofibrils, the grating order lines can be reinforced by Bragg reflection to varying degrees.

In the case of active muscle, a third effect becomes significant. Myofibrillar misalignment occurs to a large extent and results in a major decrease in the intensity of diffraction lines caused by phase randomization of diffracted light. (This is fully discussed in case III of our earlier paper [Yeh et al., 1980], and experimental evidence presented in Oba et al., 1981.)[1] The intensity decrease can be explained as the direct result of myofibrillar misalignment; no other molecular changes such as protein valency changes need to be assumed (Rüdel and Zite-Ferenczy, 1979). To summarize, we have shown that all of the observed changes in diffraction-line intensity with variation in incident angle are explicable on the basis of three interacting diffraction phenomena: first, the muscle behaving as a volume grating with diffraction the result of the different densities of A and I bands; second, the Bragg effects due to myofibril skew, and finally, upon stimulation, a large decrease in intensity of diffracted light due to myofibrillar misalignment. Thus, light diffraction studies may be used not only for measurement of sarcomere length, but also in a characterization of myofibrillar organization of the fiber at rest and during activity.

APPENDIX A

The theory (Yeh et al., 1980; see also Holmes and Blow, 1965), developed for the case where the incident angle of light was assumed to be normal to the symmetry axis of the myofibrils, has been extended in the present paper explicity to include the intensity asymmetry of the diffraction patterns when the incident angle Θ_I, is varied.

We start with the previous expression for the intensity I_ℓ (**R**) of the ℓth diffraction order from a striated muscle fiber located at a distance R from the observer.

$$I_\ell(R) = \left[\frac{|E_0|^2}{(4\pi \mathbf{R}_0)^2}\left(\frac{\omega_0}{c}\right)^4 \left|\frac{\delta\epsilon_{0_\ell}}{\epsilon_0}\right|^2\right] |F(q_p \rho a_0)|^2 |G_\ell(q_z)|^2 |H(A)|^2 \qquad \text{(A1)}$$

[1] In Eqs. 13, 19, and 22 of Yeh et al. (1980), the frequency dependency factor of $[\omega_0/c]^4$ has been inadvertently left out. For present considerations, the factors are introduced for the sake of completeness, but no alteration from this factor will enter into our discussion either in Yeh et al. (1980) or here.

where the factor in brackets ([]) represents the scattering of light from a point inhomogeneity whose relative dielectric fluctuation is $|\delta\epsilon_{0_s}/\epsilon_0|$ and the incident field has an amplitude $|E_0|$ and frequency ω_0. The second factor $|F(q_\rho a_0)|^2$ describes the meridional diffraction structure factor from an infinitely long smooth cylinder of radius a_0. The third factor,

$$|G_\ell(q_z)|^2 \equiv \left[\frac{\left(p \sin (q_z - \ell K)\frac{p}{2}\right)}{(q_z - \ell K)\frac{p}{2}}\right]^2 \tag{A2}$$

describes the diffraction of light of incident beam cross-section p by z-direction periodic index striations with the periodicity of $\Lambda = 2\pi/K$. q_z and q_ρ represent the components of the scattering wavevector $\mathbf{q}$, given by

$$\mathbf{q} = \mathbf{k}_s - \mathbf{k}_0 \tag{A3}$$

where $\mathbf{k}_0$ and $\mathbf{k}_s$ are the incident and scattered light wavevectors. The last factor,

$$|H(A)|^2 = \left[\frac{\sin \frac{NA}{2}}{\sin \frac{A}{2}}\right]^2 \tag{A4}$$

describes the interference between the N myofibrils each of which is related to its adjacent one by the skew vector $\mathbf{r}_s$, and

$$A \equiv \mathbf{q} \cdot \mathbf{r}_s \tag{A5}$$

describes the phase factor due to skew interference.

In order to apply this general formalism to the specific cases of nonnormal Θ_I, one has to relate the vector $\mathbf{q}$ to laboratory (fiber) coordinates. Consider the situation where the skewing of myfibrils occurs only in the x-z plane (Fig. A 1). Then $\mathbf{r}_s$ is represented by (see Fig. 3 of Yeh et al., 1980)

$$\mathbf{r}_s = \frac{\Delta z}{2}\hat{z} + a_0\hat{x} \tag{A6}$$

where Δz is the amount of skewing along the fiber axis, $\hat{z}$, between adjacent myofibril elements each of radius a_0 and stacked in the $\hat{x}$ direction. We wish to examine the condition where the third factor (Eq. A2) and the fourth factor (Eq. A4) are simultaneously optimized. This condition represents one where Bragg reflection from skew planes coincides with a specific order of the diffraction spectrum. From Fig. A1, we see that

$$\mathbf{k}_0 = k_0 (\sin \Theta_I \hat{z} + \cos \Theta_I \hat{x}) \tag{A7 a}$$

$$\mathbf{k}_s = k_0 (-\sin \Theta_{IR} \hat{z} + \cos \Theta_{IR} \hat{x}) \tag{A7 b}$$

where we have now specified that the $\mathbf{k}_s$ vector is directed along the right first-order diffraction maximum, Θ_{IR}, and the incident angle is Θ_I. Correspondingly, decomposing $\mathbf{q} = q_x\hat{x} + q_z\hat{z}$, we have

$$q_x = k_0 (\cos \Theta_{IR} - \cos \Theta_I) \tag{A8 a}$$

$$q_z = -k_0 (\sin \Theta_{IR} + \sin \Theta_I). \tag{A8 b}$$

Optimizing Eq. A2 requires that

$$q_z = \frac{2\pi}{\Lambda} = -k_0 (\sin \Theta_{1R} + \sin \Theta_I); \tag{A9}$$

this is the usual diffraction condition using these laboratory based angles. Optimizing Eq. A4 requires that $A = 0$. Substituting Eqs. A6 and A8 into Eq. A5 leads to the condition that

$$\tan \eta \equiv \frac{\Delta z}{2a_0} = \frac{\cos \Theta_I - \cos \Theta_{1R}}{\sin \Theta_I + \sin \Theta_{1R}}. \tag{A10}$$

Eqs. A9 and A10 suggest that for a given sarcomere length and a specific diffraction angle, unique Θ_I and η values can be found to provide Bragg enhanced diffraction of the specified order (here right first order). Θ_{1L}, the left first order does not satisfy the Bragg condition and, therefore, is not exhibited.

Several experimental consequences can be examined based on Eqs. A9 and A10. First of all, if a skew value η were fixed, a variation of the incident angle Θ_I will yield one absolute maximum. Thus there will be left-right intensity asymmetry in a scan of Θ_I (i.e., an angle scan). Second, because Eqs. A2 and A4 are both of the damped oscillatory type, secondary maxima in intensity can exist from just a single uniform skew population. Finally, because of symmetry about the skew plane, an angle scan will also yield an equal intensity maximum for the left diffraction maximum (at an incident angle Θ_I') of the same order, Θ_{1L}' at a position such that the angular difference of the maxima for the left and right of that same diffraction order will be $2\Theta_B$, or twice the Bragg reflection angle (see dotted line, Fig. A1). Furthermore, the intersection of the two asymmetrical angle scans will provide the value of the skew angle η.

This formal approach also has a very physical representation. Referring to Fig. A1, we represent the skew vector $\mathbf{r}_s$ by a plane normal to the paper tilted at an angle of η in the x-z plane. If the Bragg reflecting condition were imposed, then the angle of incidence and the angle of reflection relative to this skew plane are the same. Calling this angle Θ_B, we find that

$$\Theta_B = \Theta_I - \eta = \eta + \Theta_{1R} \tag{A11}$$

thus

$$\eta = \frac{\Theta_I - \Theta_{1R}}{2} \tag{A12}$$

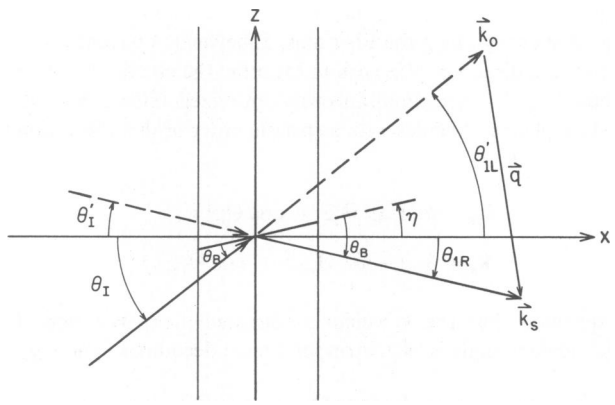

FIGURE A1 Definition of angles and coordinates used in theoretical discussion. Θ_I and Θ_I', incident angles; Θ_{1R} and Θ_{1L}', right and left Bragg diffracted orders; Θ_B is the Bragg angle for a given skew angle, η; $\mathbf{k}_0$ is the incident wavevector; $\mathbf{k}_s$ is the scattered wavevector; and $\mathbf{q}$ is the difference, $\mathbf{k}_0 - \mathbf{k}_s$.

One notes that Eq. A12 is just the small angle limit of Eq. A10, the correspondence being accurate if the discrete sarcomere skew Δz is very small compared with $2a_0$.

The form of Eqs. A9 and A10 offers the opportunity to compare theoretical predictions with experimental data. The body of this paper presents both computational data based on Eqs. A1, A9, and A10 and also direct experimental data that show excellent correspondence to our predictions.

The authors would like to express their appreciation to the National Science Foundation (grant PCM 79-03256 to R.J. Baskin) and to the National Institutes of Health (NIH, grant ROI-AM26817 to Y. Yeh) for their financial support. R.L. Lieber is an NIH predoctoral fellow.

Received for publication 17 September 1980 and in revised form 7 August 1981.

REFERENCES

Baskin, R. J., K. P. Roos, and Y. Yeh. 1979. Light diffraction study of single skeletal muscle fibers. *Biophys. J.* 28:45–64.

Holmes, K. C., and D. M. Blow. 1965. The Use of X-Ray Diffraction in the Study of Protein and Nucleic Acid Structure. Wiley-Interscience Div., John Wiley & Sons, Inc., New York.

Kawai, M. 1971. Light diffraction studies of frog striated muscle fibers. Ph.D. Thesis, Princeton University. Princeton, N.J.

Oba, T., R. J. Baskin, and R. L. Lieber. 1981. Light diffraction studies of active muscle fibers as a function of sarcomere length. *J. Muscle Res. Cell Motil.* 2:215–224.

Roos, K. P., R. J. Baskin, R. L. Lieber, J. W. Cline, and P. J. Paolini. 1980. Digital data acquisition and analysis of striated muscle diffraction patterns with a direct memory access microprocessor system. *Rev. Sci. Instrum.* 51:762–767.

Rüdel, R., and F. Zite-Ferenczy. 1979. Interpretation of light diffraction by cross-striated muscle as Bragg reflection of light by the lattice of contractile proteins. *J. Physiol. (Lond.).* 290:317–330.

Rüdel, R., and F. Zite-Ferenczy. 1980. Efficiency of light diffraction by cross-striated muscle fibers under stretch and during isometric contraction. *Biophys. J.* 30:507–516.

Yeh, Y., R. J. Baskin, R. L. Lieber, and K. P. Roos. 1980. Theory of light diffraction by single skeletal muscle fibers. *Biophys. J.* 29:509–522.